Avrupa Bilim ve Teknoloji Dergisi
Sayı 16, S. 905-914, Ağustos 2019
© Telif hakkı EJOSAT'a aittir
Araştırma Makalesi

www.ejosat.com ISSN:2148-2683

European Journal of Science and Technology
No 16, pp. 905-914, August 2019
Copyright © 2019 EJOSAT
Research Article

Double Quadrature Spatial Intensity Modulation for Visible Light Communications

Yasin Çelik[1*]

[1] Department of Electrical-Electronics Engineering, Faculty of Engineering, Aksaray University, Aksaray, Turkey (ORCID: 0000-0001-8972-9970)

(First received 25 Haziran 2019 and in final form 10 Ağustos 2019)

(**DOI:** 10.31590/ejosat.582283)

ATIF/REFERENCE: Çelik, Y. (2019). Double Quadrature Spatial Intensity Modulation for Visible Light Communications. *European Journal of Science and Technology*, (16), 905-914.

Abstract

In this paper, a new spectrally efficient space modulation technique, which is called double quadrature spatial intensity modulation (DQSIM), is proposed for multiple-input multiple-output (MIMO) visible light communication (VLC) systems. Sub-carrier intensity modulation (SCM), which ensures the use of in-phase/quadrature (I/Q) signals in intensity modulation direct detection (IM/DD) systems, is used as a digital modulation scheme. In RF, quadrature spatial modulation (QSM) transmits the I/Q signals through single or multiple antennas selected independently from each other. Furthermore, the orthogonality between I and Q components is provided for the half period of sinusoids. DQSIM utilizes these two features and transmits four fold more bits than spatial modulation (SM) via spatial constellation. SCM uses two-fold bandwidth compared to on-off keying (OOK), while DQSIM uses three fold. DQSIM outperforms benchmark modulation schemes, which are SCM-SM and pulse amplitude modulation spatial modulation (PAM-SM), at the bit error rate (BER) value of 10^{-4}. Furthermore DQSIM performance has increased with the increasing number of LEDs.

Keywords: Subcarrier intensity modulation, Spatial modulation, MIMO, VLC.

Görünür Işık Haberleşmesi için Çift Dördün Uzaysal Yoğunluk Modülasyonu

Öz

Bu çalışmada, çift dördün uzaysal modülasyon (ÇDUM) adı verilen izgesel verimi yüksek yeni bir uzaysal modülasyon tekniği çoklu-giriş çoklu-çıkış (ÇGÇÇ) görünür ışık haberleşmesi (GIH) sistemleri için önerilmiştir. Sayısal modülasyon planı olarak, eş evreli (I) ve dördün (Q) sinyallerin yoğunluk modülasyonlu direk sezim (YM/DS) sistemlerde kullanımına olanak sağlayan, alt-taşıyıcılı yoğunluk modülasyonu (AYM) kullanılmıştır. Radyo frekans (RF) haberleşmesinde dördün uzamsal modülasyon (DUM) I/Q sinyallerini her biri diğerinden bağımsız olarak seçilmiş antenlerden iletir. Dahası I/Q sinyalleri arasındaki diklik sinüzoidal sinyallerin yarım periyodunda da korunmaktadır. ÇDUM bu iki özelliği kullanarak uzamsal modülasyonun (UM) dört katı biti uzaysal boyutta iletir. AYM, aç-kapa anahtarlamaya (AKA) kıyasla iki kat bant genişliği kullanırken, ÇDUM üç kat kullanır. Bu çalışmada ÇDUM performansı AYM-UM ve darbe genlik modülasyonlu uzamsal modülasyon (DGM-UM) ile karşılaştırılmış ve daha iyi bir performans sergilediği gösterilmiştir. Ek olarak, verici taraftaki LED sayısı arttıkça ÇDUM performansı artmaktadır.

Anahtar Kelimeler: Alt-taşıyıcılı yoğunluk modülasyonu. Uzamsal modülasyon, ÇGÇÇ, GIH.

[*] Corresponding Author: [1]Department of Electrical and Electronics Engineering, Faculty of Engineering, Aksaray University, Aksaray, Turkey, ORCID: 0000-0001-8972-9970, yasincelik@aksaray.edu.tr

1. Introduction

Visible light communication (VLC) is an up-and-coming technology for short and medium-range wireless communications. It comes out as a complementary solution for present communication systems and helps for getting over the spectrum shortage problem in short and medium-range wireless communications. It also has several advantages that can not be achieved by radio frequency (RF) systems, for example, communication in electromagnetic sensitive areas, immunity to eavesdropping, be used both for illumination and communication, etc. [1, 2].

In RF communication systems, in-phase/quadrature (I/Q) data and modulation schemes are prevalent because of their efficiency in spectrum and power. However, complex and negative components of the I/Q data are not convenient for transmitting over intensity modulation direct detection (IM/DD) systems, and also over VLC systems. Thus, conventional VLC communication systems were based on baseband pulsed modulations [3]. Later on, orthogonal frequency division multiplexing (OFDM) was adapted for VLC systems by transforming the complex-bipolar signal to real-unipolar signal through some operations, such as, Hermitian symmetry, DC-bias etc.. However, such operations are performed at the cost of decreasing spectral efficiency (SE) and/or energy efficiency. Furthermore, peak to average power ratio (PAPR) is a main drawback for OFDM and its variants [4].

As an alternative to baseband modulations and optical OFDM variants, subcarrier intensity modulation (SCM) has also been proposed for IM/DD systems [5, 6]. SCM supplies efficient modulation schemes, such as, quadrature amplitude modulation (QAM), phase shift keying (PSK), etc., without PAPR problem and it also ensures the use of I/Q data in VLC systems. SCM is composed of sine and cosine signal pair and a DC bias signal which assures that the sum of sinusoidal signals is positive during all transmission period. As a drawback, due to its band-pass form, SCM needs twice the bandwidth of on-off keying (OOK) modulation [7].

In order to increase SE, multiple-input multiple-output (MIMO) technique is a well-known concept in RF. It is carried out by simultaneously transmitting independent data streams from multiple transmitters to multiple receivers. In general, multiple LEDs are located in a distributed manner with the intention of illumination purposes in indoor environments. Therefore, LED locations in a room naturally supports the MIMO structure for VLC systems [8]. Thus, MIMO communication techniques are easily adapted for VLC systems in order to overcome the SE loss which caused by generation of the real-unipolar signal.

Spatial multiplexing (SMX), repetition coding (RC), and space modulation techniques (SMT), especially spatial modulation (SM), are the well-researched MIMO techniques for VLC systems [9, 10]. SMTs are relatively new and efficient MIMO transmission schemes that exploit the differences between channel gains to modulate additional information bits [11]. Spatial modulation (SM) which is the first popular concept for SMT was proposed by Mesleh et al. in 2008. In SM, one of the transmit antenna is activated at each symbol period and all others are turned off. This scheme is implemented with a single RF-chain which assures reduced implementation cost, decreased computational complexity, eliminated inter-channel interference (ICI), and increased energy efficiency. As a result of activating single transmit antenna at each symbol period, $log_2(N_t)$ bits are transmitted by spatial constellation [11].

Thanks to the orthogonality between I and Q components of the sinusoidal signal pairs, quadrature spatial modulation (QSM) was proposed in RF. Like SM, QSM is also implemented with a single RF chain, but two antennas may be active in one symbol period due to the I and Q spatial symbols which are independent of each other. Therefore, spatial constellation size and also the number of spatially transmitted bits is doubled in QSM. Thus, total SE of the QSM is given by $(log_2(M) + 2\ log_2(N_t))$ bit per channel use (bpcu) where M is the signal constellation size [12, 13].

The orthogonality between I and Q components is also provided in the half period of sinusoids. With the aid of this property, double quadrature spatial intensity modulation (DQSIM) is proposed for MIMO VLC systems in this paper. DQSIM is the spectrally efficient version of the QSIM that allows switching between LEDs at a rate of twice the symbol rate. Therefore, sinusoidal signal pairs are transmitted separately by the LEDs chosen according to the spatial symbols at a rate of twice the symbol rate. So the number of spatially modulated bits is doubled and the SE of DQSIM is given by $(log_2(M) + 4\ log_2(N_t))$ bpcu. DQSIM can also be designed with a single RF-chain and utilizes the advantages of this feature.

2. Material and Method

2.1. System Model

In this paper, an indoor VLC system with multiple LEDs and PDs is considered. The number of LEDs and PDs are donated by N_t and N_r, respectively. It is assumed that the LEDs are perfectly synchronized and temporal delay is negligible between multiple links, so the considered system model has no time dispersion. The block diagram of the proposed DQSIM transmitter and receiver is shown in Fig. 1.

2.1.1. DQSIM Transmitter Model

At the transmitter side, the incoming bits are separated into five groups. The first group contains $log_2(M)$ bits, which is used to choose the digitally modulated symbol. The other four groups separately contain $log_2(N_t)$ bits and each one is used to choose a spatial symbol independently. Among these four groups, the first two, T_{IF} and T_{QF}, determine the indexes of the active LED or LEDs at the first phase of symbol period and the last two, T_{IS} and T_{QS}, determine the indexes of the active LED or LEDs at the second phase of symbol period.

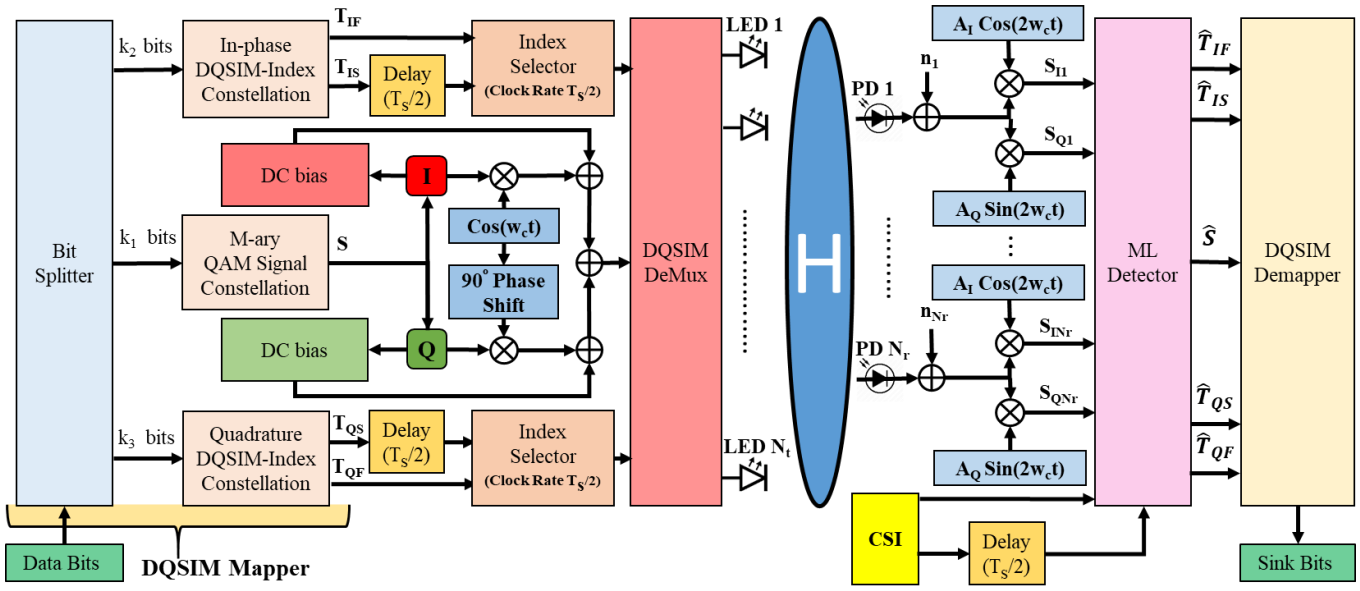

Figure 1. Block diagram of the proposed DQSIM transmitter and receiver.

The transmitted signal is obtained from SCM, which is the sum of sinusoidal signal pairs and a DC signal. The DC signal must ensure that the total electrical signal is always positive [5]. Since the constant DC signal reduces the power efficiency of the SCM, the power-efficient form of the SCM using symbol-by-symbol DC bias is proposed [15]. This form of SCM is considered in this study and quadrature amplitude modulation (QAM) is used as the modulation scheme. At the transmitter side, orthonormal base functions in half period are given as;

$$\phi_{1F}(t) = \sqrt{\frac{2}{T_s}}\cos(2\pi f_c t)\, rect\left(\frac{2t}{T_s} - \frac{T_s}{4}\right), \tag{1}$$

$$\phi_{1S}(t) = \sqrt{\frac{2}{T_s}}\cos(2\pi f_c t)\, rect\left(\frac{2t}{T_s} - \frac{T_s}{2}\right), \tag{2}$$

$$\phi_{2F}(t) = \sqrt{\frac{2}{T_s}}\sin(2\pi f_c t)\, rect\left(\frac{2t}{T_s} - \frac{T_s}{4}\right), \tag{3}$$

$$\phi_{2S}(t) = \sqrt{\frac{2}{T_s}}\sin(2\pi f_c t)\, rect\left(\frac{2t}{T_s} - \frac{T_s}{2}\right), \tag{4}$$

where T_s is the symbol interval and $f_c = 1/T_s$ is the subcarrier frequency. Rectangular window function, $rect(t)$, is defined as;

$$\text{rect(t)} = \begin{cases} 1, & -1/2 \le t \le 1/2, \\ 0, & o/w. \end{cases} \tag{5}$$

Consequently, before adding DC the transmitted signals in the first and second phase are expressed as follows;

$$\text{x}_\text{F}(\text{t}) = \{S_{l\Re}\}_F \phi_{1F}(t) + \{S_{l\Im}\}_F \phi_{2F}(t), \tag{6}$$

$$\text{x}_\text{S}(\text{t}) = \{S_{l\Re}\}_S \phi_{1S}(t) + \{S_{l\Im}\}_S \phi_{2S}(t), \tag{7}$$

here, $l = \{1,2,\ldots,M\}$ and M is the constellation size of the digitally modulated symbols. $S_{l\Re}$ and $S_{l\Im}$ are obtained from the symbol set S and $S = \{S_1, S_2, \ldots, S_M\}$. S is the constellation of QAM with the size of M, so $S_l = S_{l\Re} + jS_{l\Im}$. The transmitted vector at the first and the second phases consist of half period of sinusoidal signal pairs. Furthermore, one complex symbol is sent in one symbol period, so the first phase symbol is equal to the second phase symbol, $S_{lF} = S_{lS}$. According to the T_{IF}, T_{QF}, T_{IS}, and T_{QS} indices, the active LEDs are determined for the first and second phases. After that, $x_F(t)$ and $x_S(t)$ signals are transmitted from the active LEDs, respectively. At the output of the DQSIM demultiplexer, the transmitted signal vector is given as $\mathbf{x} = [\mathbf{x}_F\ \mathbf{x}_S]$, where $\mathbf{x}_F = [0, S_{l\Im}, S_{l\Re}, \ldots 0]^T$ and $\mathbf{x}_S = [S_{l\Im},$

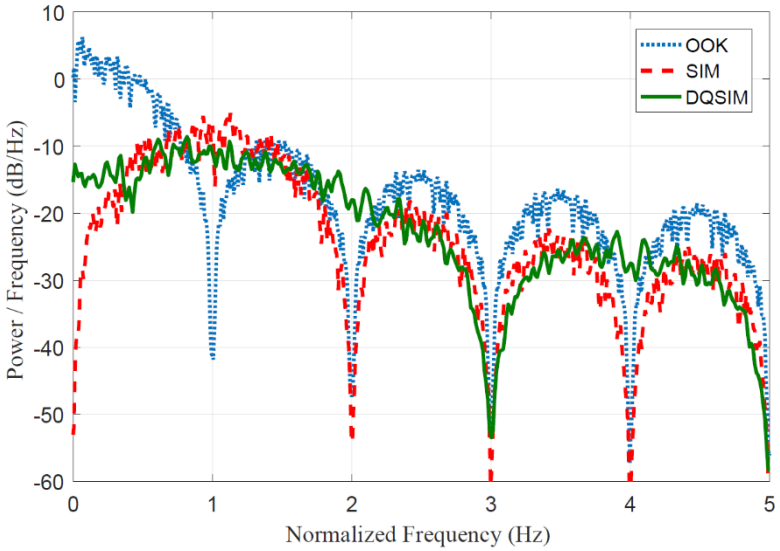

Figure 2. Bandwidth comparison between OOK, SIM and DQSIM.

$S_{l\Re}$, 0, …, 0]^T are N_tx1 vectors with the non-zero elements at the T_{IF}, T_{QF}, T_{IS}, and T_{QS} index positions. The transmitted signal, $x(t)$, is obtained as the sum of inphase, quadrature and DC components and used to drive the LEDs.

To make a fair comparison between modulation schemes, the system bandwidth and the transmission powers used must be the same. In addition, it is common to use the first null bandwidth to measure the bandwidth of the transmission systems. In Fig. 2, the frequency domain representation of the OOK, SCM and DQSIM schemes are given. As shown in Fig. 2, the first null bandwidth usage of the OOK scheme, which is 2-PAM, is minimum. SCM scheme requires twice as much bandwidth as the OOK, and DQSIM requires three-fold the bandwidth of OOK. The bandwidth usage is taken into account in simulations to achieve the same spectral efficiency.

Some bit mapping examples of the proposed scheme for $N_t = 4$ and $M = 4$ is shown in Table I. This table illustrates the transmitted signal (**x**) for corresponding data bits. $\{S_l\}_F$ stands for the first half period of the S_l and $\{S_l\}_S$ corresponds to the second half period of the S_l. In addition, S_l consists of the sum of real and imaginary parts as ($S_{l\Re} + S_{l\Im}$). The sum of k_1, k_2, and k_3, which is equal to the $\log_2(MN_t^4)$ bits, are sent during each symbol period. The average electrical energy consumed at the active LED or LEDs in every channel use is equal to Es.

Table 1. Examples of the DQSIM with SE of 10 bpcu for Nt = 4 and M = 4.

Incoming Bits			**Transmitted Data**							
			***First Phase* (x_F)**				***Second Phase* (x_S)**			
k_1	k_2	k_3	***LED1***	***LED2***	***LED3***	***LED4***	***LED1***	***LED2***	***LED3***	***LED4***
00	0101	0110	0	$\{S_1\}_F$	0	0	0	$\{S_{1\Re}\}_S$	$\{S_{1\Im}\}_S$	0
01	1010	1001	0	0	$\{S_2\}_F$	0	0	$\{S_{2\Im}\}_S$	$\{S_{2\Re}\}_S$	0
10	1111	0011	$\{S_{3\Im}\}_F$	0	0	$\{S_{3\Re}\}_F$	0	0	0	$\{S_3\}_S$
11	0000	1100	$\{S_{4\Re}\}_F$	0	0	$\{S_{4\Im}\}_F$	$\{S_4\}_S$	0	0	0
10	0001	1000	$\{S_{3\Re}\}_F$	0	$\{S_{3\Im}\}_F$	0	$\{S_{3\Im}\}_S$	$\{S_{3\Re}\}_S$	0	0
00	0011	1111	$\{S_{1\Re}\}_F$	0	0	$\{S_{1\Im}\}_F$	0	0	0	$\{S_1\}_S$
01	0111	1110	0	$\{S_{2\Re}\}_F$	0	$\{S_{2\Im}\}_F$	0	0	$\{S_{2\Im}\}_S$	$\{S_{2\Re}\}_S$
11	1101	0010	$\{S_{4\Im}\}_F$	0	0	$\{S_{4\Re}\}_F$	0	$\{S_{4\Re}\}_S$	$\{S_{4\Im}\}_S$	0
11	1111	1111	0	0	0	$\{S_4\}_F$	0	0	0	$\{S_4\}_S$
00	0000	0000	$\{S_1\}_F$	0	0	0	$\{S_1\}_S$	0	0	0
01	1100	1100				$\{S_2\}_F$	$\{S_2\}_S$			
10	0110	0011	$\{S_{3\Im}\}_F$	$\{S_{3\Re}\}_F$					$\{S_{3\Re}\}_S$	$\{S_{3\Im}\}_S$

2.1.2 MIMO VLC Channel Model

In this study, direct line-of-sight (LOS) channel characteristic is assumed between LEDs and PDs for indoor VLC. **H** is the N_r x N_t MIMO channel matrix and the channel coefficient of the optical link between the transmitter j and the receiver i is represented by h_{ij} which is the element in the i^{th} row and j^{th} column of the matrix **H.** The placement of LEDs and PDs in x-y plane is given in Fig. 3a and the link geometry is shown in Fig. 3b, where α_{ij} and β_{ij} are defined as the angles between the normal and the LOS link for LED and PD,

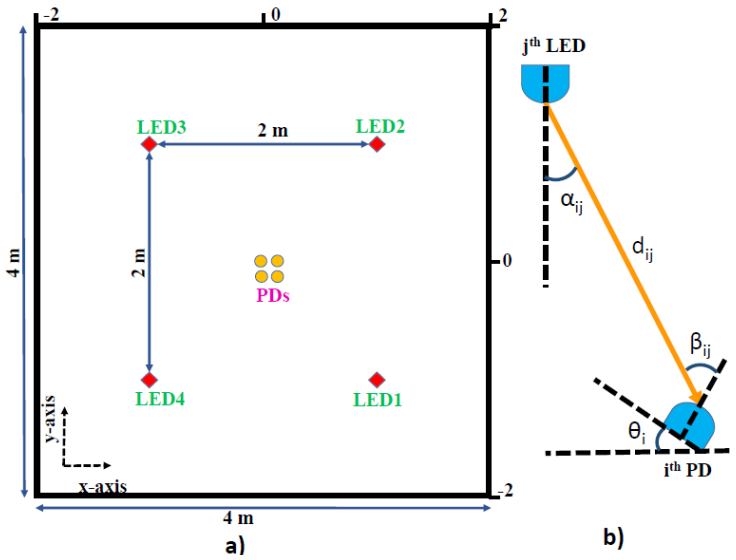

Figure 3. a) Positions of LEDs and PDs in x - y plane, b) Link geometry.

respectively. Angular diversity receiver (ADR) is a compact receiver type considered in this work. Pyramid ADR is designed according to the principles given in [14]. For this receiver type, the elevation angle of the i^{th} PD is considered as θ_i which is shown in Fig. 3b. In particular, the azimuth angle, ϕ, is considered as $0°$, and the elevation angle, θ, is taken into account as $60°$ for getting the best channel conditions.

Assuming the LEDs have Lambertian radiation pattern, the MIMO channel coefficient h_{ij} will be given as following [14],

$$h_{ij} = \begin{cases} \frac{(m+1)A}{2\pi d_{ij}^2} cos^m(\alpha_{ij}) \cos(\beta_{ij}), & \left|\frac{\beta_{ij}}{FOV}\right| \leq 1, \\ 0, & otherwise. \end{cases} \tag{8}$$

In (8), since the LED semi-angle (at half power) is considered as 60°, Lambertian emission order, m, is equal to 1. d_{ij} is the distance in meters from j^{th} LED to i^{th} PD. α_{ij} is the angle between the link from j^{th} LED to i^{th} PD and the normal of j^{th} LED. Similarly, β_{ij} is the angle between the link from j^{th} LED to i^{th} PD and the normal of i^{th} PD. FOV is the field of view angle of the PD, and A is the active area of PD which is 15 mm^2 for Centronic OSD15-E PDs [14].

The room sizes for our indoor scenario are considered as 4 m, 4 m, and 3 m in x, y, and z directions, respectively. The top view of the indoor place in x - y plane is showed in Fig. 3a. The LEDs are placed at a height of 2.7 m in the z-direction and to the diagonals of the x - y plane of the room with the same distances between each other.

At the receiver side, multiple PDs are designed in a compact manner and formed the ADR unit. This unit is located at the center of the room with a height of 0.8 m in the z-direction, which corresponds to (0,0,0.8) location in (x, y, z) coordinates. Because of the receiver units are designed in a compact manner, the distances between the PDs are negligible, so the positions of the PDs are assumed to be same as the position of the ADR unit.

2.1.3 DQSIM Receiver Model

Light intensity, which consists modulated signal with DC-bias is detected by the PDs in the ADR unit. After electrical-to-optical conversion, the received signal vector in one symbol period is described as follows,

$$\boldsymbol{y} = \eta\rho\boldsymbol{H}\boldsymbol{x} + \boldsymbol{n}, \tag{9}$$

where η is the electrical-to-optical conversion coefficient and ρ is the photo-detector sensitivity. Without loss of generality we assume $\eta\rho = 1$. The shot and the thermal noises occured at the receiver are modeled as additive white Gaussian noise (AWGN) which is independent of the transmitted signal and added to the received signal in the electrical domain. $\mathbf{n}$ is N_r dimensional Gaussian random variable with zero mean and has a variance of σ_n^2. The modulated data, consists of indice symbols as well as digitally modulated symbols, is obtained with the help of orthogonality between sinusoidal signal pairs. Since the received signal has a DC-bias at half symbol rate, matched filter can not reach maximum SNR, which is defined as $E[\mathbf{x}^T\mathbf{x}]/\sigma_n^2$. Here, E[.] is the expectation operator. In order to retrieve indice information at half symbol rate, a high pass filter approach is proposed for DQSIM scheme. The received signal at the i^{th} PD can be divided into two parts as $\mathbf{y}_{F(i)}$ and $\mathbf{y}_{S(i)}$ which correspond to the first half of symbol period (first phase) and the second half of symbol period (second phase), respectively. are defined as following,

$$y_{F(i)}(t) = DC_F(t) + h_{IF(i)} \{S_{l\Re}\}_F \phi_{1F}(t) + h_{QF(i)} \{S_{l\Im}\}_F \phi_{2F}(t) + n_{F(i)}, \tag{10}$$

$$y_{S(i)}(t) = DC_S(t) + h_{IS(i)}\{S_{l\Re}\}_S\phi_{1S}(t) + h_{QS(i)}\{S_{l\Im}\}_S\phi_{2S}(t) + n_{S(i)}. \quad (11)$$

Here, $i = 1, 2, \ldots, N_r$ corresponds to the receiver indice. $h_{IF(i)}$ and $h_{IS(i)}$ indicate the channel coefficients between active LED and i^{th} PD for inphase carrier at first and second phases, respectively. Also, $h_{QF(i)}$ and $h_{QS(i)}$ are the channel coefficients for quadrature carrier in the same manner. $DC_F(t)$ and $DC_S(t)$ are the direct current in the transmitted signal for the first and second phases, respectively. $n_{F(i)}$ and $n_{S(i)}$ are the zero mean Gaussian random variables at the i^{th} PD with a variance of $\sigma^2 = N_0/2$ per dimension.

The inphase and quadrature components of the received signal can be retrieved by filtering received signal with high frequency sinusoidals. In order to obtain the information carried with inphase carrier, a high frequency quadrature signal can be used for filtering quadrature and DC components. And also, getting the information carried with quadrature carrier, a high frequency inphase signal can be used for filtering inphase and DC components. Twice the carrier frequency is enough for high frequency component to provide orthogonality between sinusoidal pairs. Thus, the estimated inphase and quadrature signals for the first and second phases at the i^{th} PD are obtained as following;

$$\hat{y}_{IF(i)} = \int_0^{\frac{T_S}{2}} y_{F(i)}(t)\sin(4\pi f_c t)\, d(t), \quad (12)$$

$$\hat{y}_{QF(i)} = \int_0^{\frac{T_S}{2}} y_{F(i)}(t)\cos(4\pi f_c t)\, d(t). \quad (13)$$

$$\hat{y}_{IS(i)} = \int_{\frac{T_S}{2}}^{T_S} y_{S(i)}(t)\sin(4\pi f_c t)\, d(t), \quad (14)$$

$$\hat{y}_{QS(i)} = \int_{\frac{T_S}{2}}^{T_S} y_{S(i)}(t)\cos(4\pi f_c t)\, d(t). \quad (15)$$

After some simple derivations and normalization with $\sqrt{2/T_S}$ general forms for estimated inphase and quadrature signal at the i^{th} PD is given as;

$$\hat{y}_{IF(i)} = \frac{4}{3}h_{IF(i)}\{S_{l\Re}\}_F + \hat{n}_{IF(i)}, \quad (16)$$

$$\hat{y}_{QF(i)} = \frac{-2}{3}h_{QF(i)}\{S_{l\Im}\}_F + \hat{n}_{QF(i)}, \quad (17)$$

$$\hat{y}_{IS(i)} = \frac{4}{3}h_{IS(i)}\{S_{l\Re}\}_S + \hat{n}_{IS(i)}, \quad (18)$$

$$\hat{y}_{QS(i)} = \frac{-2}{3}h_{QS(i)}\{S_{l\Im}\}_S + \hat{n}_{QS(i)}, \quad (19)$$

where, $\hat{n}_{IF(i)}, \hat{n}_{QF(i)}, \hat{n}_{IS(i)}$, and $\hat{n}_{QS(i)}$ are the zero mean Gaussian random variables at the i^{th} PD with a variance of $\sigma^2 = N_0/4$ per dimension. The coefficients in the high pass filtering process of Fig. 1, A_I and A_Q, are obtained from above equations as *3/4* and *3/2,* respectively. Finally, the N_Rx*1* received signal is given as;

$$\hat{\boldsymbol{y}} = [\,[\widehat{y}_{IF1} + j\hat{y}_{QF1}, \hat{y}_{IS1} + j\hat{y}_{QS1}], \ldots, [\widehat{y}_{IFN_R} + j\hat{y}_{QFN_R}, \hat{y}_{ISN_R} + j\hat{y}_{QSN_R}]\,]^T. \quad (20)$$

The received signal is then processed by a maximum likelihood (ML) decoder to jointly estimate the spatial symbols and the digitally modulated symbol as,

$$\left(\widehat{\boldsymbol{S}}, \widehat{\boldsymbol{T}}_{IF}, \widehat{\boldsymbol{T}}_{QF}, \widehat{\boldsymbol{T}}_{IS}, \widehat{\boldsymbol{T}}_{QS}\right) = \underset{S, T_{IF}, T_{QF}, T_{IS}, T_{QS}}{\operatorname{argmin}} \left(\left|\left|\hat{\boldsymbol{y}} - \boldsymbol{H}\boldsymbol{x}\right|\right|_F^2\right), \quad (21)$$

where F denotes the Frobenious norm. The computational complexity of considered schemes are presented in Table 2.

Table 2. Computational complexity of considered schemes

Scheme	Complexity	Complexity in terms of SE
PAM-SM	MN_t2N_r	$2^{SE}2N_r$
SCM-SM	$2MN_t3N_r$	$2^{2SE}6N_r$
DQSIM	$2MN_t^43N_r$	$2^{3SE}6N_r$

3. Results and Discussion

3.1. Simulation Results

In this section, the BER performance of the considered modulation schemes for indoor VLC systems with compact ADR unit is showed. SM scheme is used as a MIMO plan with the fixed mean emitted electrical power in one symbol period. Furthermore, comparisons are made at the same spectral efficiencies for all scenarios, except DQSIM at spectral efficiency value of 3 bits/s/Hz. The spectral efficiency of DQSIM is assumed to be 3.33 bits/s/Hz with N_t=4 and M=4 in this scenario. In our simulations, the SNR value is indicated by the electrical E_b/N_0 in dB.

Since comparisons are made at the same spectral efficiency of 3 bits/s/Hz, the modulation sizes of PAM and SCM for SM scheme are considered as 2 and 16, respectively. When the number of LEDs is 4 at the transmitter side, it is not possible to obtain 3 bits/s/Hz spectral efficiency with an integer M value. Thus, the modulation size of DQSIM is assumed to be 4 to achieve the spectral efficiency of 3.33 bits/s/Hz. As for spectral efficiency of 5 bits/s/Hz, modulation sizes of 4, 128, and 8 are needed for PAM, SCM, and DQSIM, respectively. In this indoor scenario, the number of LEDs is 8 at the transmitter side. All of the parameters used in indoor VLC simulation are summarized in Table 3.

Table 3. Simulation parameters for indoor MIMO VLC with ADR unit.

Length (X)	4 m
Width (Y)	4 m
Height (Z)	3 m
No. of LEDs (N_t)	4, 8
LED distance from the roof	0.3 m
Distance between LEDs	2 m
Transmitter elevation angle	- 90°
Transmitter azimuth angle	0°
Half power semi-angle ($\Phi_{1/2}$)	60°
Mode number (n)	1
PD height from the floor	0.8 m
Receiver elevation angle	60°
Receiver azimuth angle	0°
Responsivity	1 A/$\sqrt{W}$
Area of the detector (A)	1.5 x 10^{-4} m^2
FOV	85°
No. of PDs (N_r)	4

Figure 4 shows the BER performances of PAM, SCM, and DQSIM schemes for SM-MIMO plan at the spectral efficiency of 3 bits/s/Hz. The receiver is located at the center of the room. The proposed scheme and PAM-SM outperform the SCM-SM nearly 4 dB at the BER value of 10^{-4} and has the same performance at this BER value. However, DQSIM has the advantage of 0.33 bits/s/Hz spectral

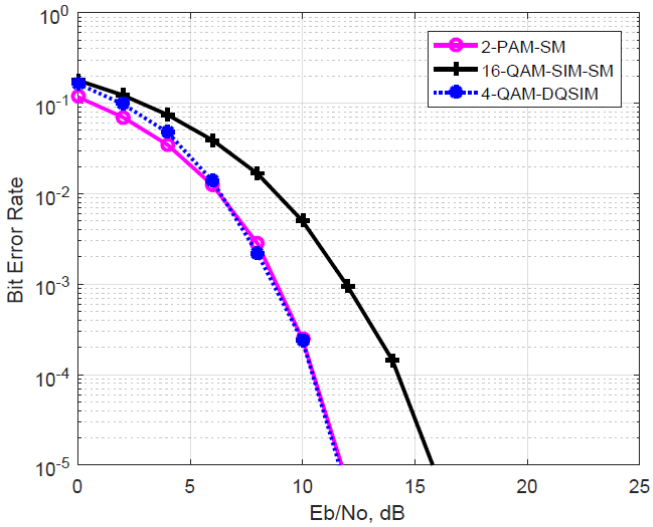

Figure 4. BER simulation results for 4 x 4 MIMO DQSIM scheme SE value of 3.33 bits/s/Hz for DQSIM and 3 bits/s/Hz for others

efficiency over PAM-SM for this configuration. The BER of 10^{-4} is sufficient to ensure reliable communicationwith error correcting codes [16].

In Figure 5, the BER performances of PAM, SCM, and DQSIM were evaluated using 8 LEDs at the transmitter side. In this indoor scenario, the spectral efficiency of 5 bits/s/Hz is achieved and the receiver is also located at the center of the room. DQSIM performs better than the benchmark modulations with the SM scheme. It outperforms SCM-SM nearly 7 dB and PAM-SM 0.5 dB at the BER value of 10^{-4}. As a result, DQSIM performance has increased with increasing number of transmitters. The DQSIM scheme stands out in this scenario and overcomes the disadvantage of bandwidth. SCM-SM has the worst BER performance in both two scenarios. The BER performance of PAM-SM is close to DQSIM. However, PAM's power efficiency decreases with an increase in M.

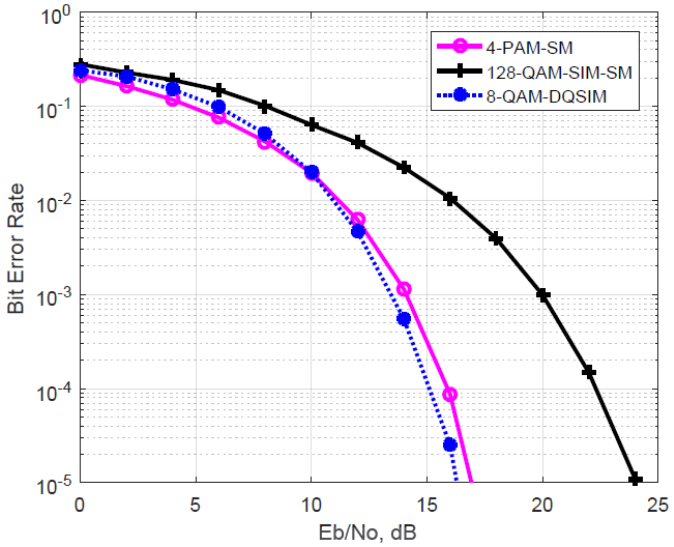

Figure 5. BER simulation results for 8 x 4 MIMO DQSIM scheme with Nt = 8 and and SE value of 5 bits/s/Hz

4. Conclusions and Recommendations

DQSIM technique has been proposed as a spectrally efficient modulation scheme for indoor MIMO VLC systems. It has been shown via Monte Carlo simulations that, its SNR advantage increases more than SM schemes with the increasing number of LEDs. This suggests that DQSIM constellation with large number of LEDs would be suitable for indoor VLC scenarios. In addition, to overcome the drawback that the number of transmit antennas has to be an integer exponent of 2, the generalized schemes will be used [17]. In generalized schemes, a constant number of transmit antennas is activated in each symbol period and the same signal is transmitted from all of the enabled antennas. Thus, combination of active antennas available at transmitter increases the number of index bits modulated to the spatial domain.

References

[1] Khan, L.U. 2017. Visible light communication: Applications, architecture, standardization and research challenges, Digital Communications and Networks, 3, 2, pp. 78-88. https://doi.org/10.1016/j.dcan.2016.07.004

[2] Jovicic, A. Li, J. and Richardson, T. 2013. Visible light communication: Opportunities, challenges and the path to market IEEE Commun. Mag. 51, 12, pp. 26-32. https://doi.org/10.1109/MCOM.2013.6685754

[3] Dimitrov, S. and Haas, H. 2015. Principles of LED Light Communications, Cambridge University Press, Cambridge, UK.

[4] Armstrong, J. 2009. OFDM for Optical Communications, IEEE Journal of Lightwave Tech., 27, 3, pp. 189-204. https://doi.org/10.1109/JLT.2008.2010061

[5] Barry, J. R. 1994. Wireless Infrared Communications, Norwell, MA Kluwer.

[6] Islim, M. S. and Haas, H. 2016. Modulation Techniques for Li-Fi, ZTE Communications, 14, 2, pp. 29-40. https://www.research.ed.ac.uk/portal/en/publications/modulation-techniques-for-lifi

[7] Celik, Y. and Akan, A. 2018. Subcarrier intensity modulation for MIMO visible light communications, Optics Communications, 412, pp. 90-101. https://doi.org/10.1016/ j.optcom.2017.12.002

[8] Zeng, L. and et al. 2009. High Data Rate Multiple Input Multiple Output (MIMO) Optical Wireless Communications Using White LED Lighting, IEEE Journal on Selected Areas in Comm., 27, 9, pp. 1654-1662. https://doi.org/10.1109/ JSAC.2009.091215

[9] Mesleh, R. and et al. 2011. Optical Spatial Modulation, IEEE/OSA Journal of Optical Communications and Networking, 3, 3, pp. 234-244. https://doi.org/10.1364/ JOCN.3.000234

[10] Fath, T. and Haas, H. 2013. Performance comparison of MIMO techniques for optical wireless communications in indoor environments, IEEE Transactions on Communications, 61, 2, pp. 733–742. https://doi.org/10.1109/ TCOMM.2012.120512.110578

[11] Mesleh, R. and et. al. 2008. Spatial modulation, IEEE Trans. Veh. Technol., 57, 4, pp. 2228-2241. https://doi.org/10.1109/TVT.2007.912136

[12] Mesleh, R., Ikki, S., and Aggoune H. 2015. Quadrature spatial modulation, IEEE Trans. Veh. Technol., 64, 6, pp. 2738-2742. https://doi.org/10.1109/TVT.2014.2344036

[13] Mesleh, R. and Alhassi, A. 2018. Space Modulation Techniques, Wiley, 1th Ed., Hoboken, USA.
[14] Nuwanpriya, A. and et al. 2015. Indoor MIMO visible light communications: Novel angle diversity receivers for mobile users, IEEE Journal on Selected Areas in Communications, 33, 9, pp. 1780-1792.
[15] You, R. and Kahn, J. M. 2001. Average power reduction techniques for multiple-subcarrier intensity-modulated optical signals, IEEE Transactions on Communications, 49, 12, pp. 2164-2171. https://doi.org/10.1109/26.974263
[16] Y. Qiu and et al., 2018. Visible Light Communications Based on CDMA Technology, IEEE Wireless Communications, 25, 2, pp.178-185.
[17] A. Younis and et al., 2010. Generalized spatial modulation, Conf. Rec. Asilomar Signals, Syst., Comput., pp. 1498-1502, Pacific Grove, CA, USA.